Magnetic flower-like Fe-doped CoO nanocomposites with dual enzyme-like activities for facile and sensitive determination of H_2O_2 and dopamine

Jiajia Lian[a], Yanlei He[a], Ning Li[a], Pei Liu*[,b], Zhenxue Liu[a], and Qingyun Liu*[,a]

[a] College of Chemical and Biological Engineering, Shandong University of Science and Technology, Qingdao 266590, China

[b] College of Chemistry and Chemical Engineering; Analysis and Testing Center, Henan Polytechnic University, Jiaozuo 454000, China.

*** Corresponding Author**

E-mail: qyliu@sdust.edu.cn

Tel: +86 0532 86057757

Experimental section

Characterizations

X-ray powder diffraction (XRD) patterns were measured on an X-ray diffractometer (Rigaku D/Max-rB) with an interval of 0.02° at a scanning step of 8° min^{-1}. The BET specific surface area and BJH pore size distribution were determined at 77 K on a fully automatic specific surface area and porosity analyzer (MIKE Micromeritics ASAP2460) after degassing the samples at 120 °C for 12 h. Scanning electron microscopy (SEM) images and elemental dispersive spectroscopy (EDS) were determined on a FEI APREO microscope operating at 20 kV. High resolution transmission electron microscopy (HRTEM) images and elemental mapping images were collected on a TEM system (FEI Tecnai G2 F20) operating at 200 kV. X-ray photoelectron spectra (XPS) were measured by using a Multifunctional imaging electron spectrometer (Thermo ESCALAB 250Xi) with Al Kα radiation operating at 250 W.

Peroxidase-like activity

The peroxidase-like activity of Fe-CoO NCs was initially evaluated for TMB oxidation with H_2O_2 as additive. In short, 200 μL catalyst (0.3 mg mL^{-1}), 200 μL H_2O_2 solution (200 mM) and 200 μL TMB solution (1 mM) were added into 1400 μL buffer (pH of 4.0), respectively. After reacting for 60 s at room temperature (25 ± 2 °C), the specific absorbance of oxidized TMB (ox-TMB) at 652 nm was measured on a UV-visible spectrophotometer (Persee Analytics, TU1810). The 0.15Fe-CoO NCs possessed the highest peroxidase-mimicking activity. Then, control experiments were

conducted to confirm the dual enzyme-like activities of 0.15Fe-CoO NCs. Furthermore, the influences of pH and temperature were investigated to achieve the best performance of 0.15Fe-CoO nanozymes.

Kinetic tests

The steady kinetics of 0.15Fe-CoO NCs as peroxidase mimics were studied by varying the concentration of one substrate and keeping that of another a constant. The initial reaction velocity (v) can be obtained by linear fitting the specific absorbances versus reaction times. The relationship of v against the substrate concentration (C) should well match the typical second-order Michaelis-Menten (M-M) curve. The M-M constant (K_m) and maximum initial reaction rate (V_m) can be calculated from the slope and intercept of the evolved double reciprocal curve: $v^{-1} = (K_m/V_m)C^{-1} + V_m^{-1}$. A smaller K_m value means a higher affinity between mimics and the substrate.

Determination of H_2O_2 and DA

Based on the superior peroxidase-like activity of 0.15Fe-CoO NCs, a colorimetric sensor was developed for sensitive and selective detection of H_2O_2 and DA. The LOD value towards H_2O_2 was obtained by varying the H_2O_2 from 1 to 100 μM. The selectivity was studied in comparison with various interferences which has ten times higher concentration than that of H_2O_2, including metal ions, carbohydrates and amino acids. Similarly, after reacting for 60 s, DA was added into 0.15Fe-CoO+H_2O_2+TMB system, then immediately measuring the absorbance at 652 nm. Due to the inhibition of DA for the catalytic oxidation of TMB, the absorbance difference (ΔA) before and after adding DA should be linearly related with the DA

concentration within a certain range. And the sensitivity and selectivity of the proposed sensor toward DA were also investigated.

Mechanism research

To understand the plausible catalytic mechanism of 0.15Fe-CoO NCs, fluorescence probe experiments were performed on a fluorescence spectrophotometer (HACHI, F-4600 FL) with the excitation wavelength of 315 nm. The non-fluorescent PTA easily reacts with •OH to produce the highly fluorescent 2-hydroxy terephthalic acid (HTA) which has the maximum fluorescence intensity at around 432 nm. Therefore, PTA can be applied as the fluorescence probe to confirm whether the generation of •OH was catalyzed by 0.15Fe-CoO NCs or not. Moreover, radical trapping experiments were performed by using IPA, PBQ, and EDTA-2Na to scavenge •OH, $•O_2^-$, and hole (h^+), respectively.

Results and discussion

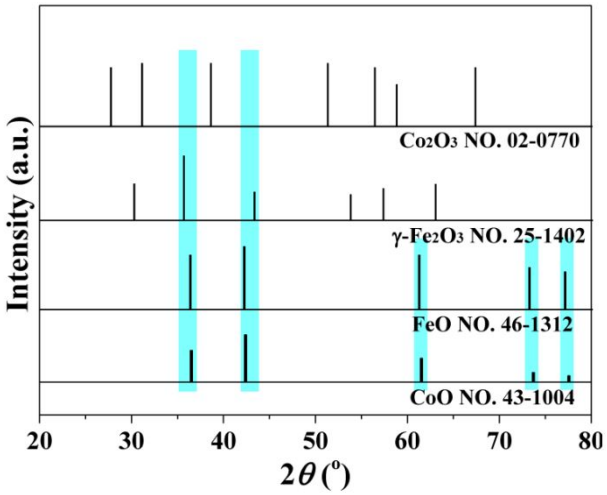

Figure S1. XRD standard cards of CoO, FeO, and γ-Fe_2O_3, and Co_2O_3.

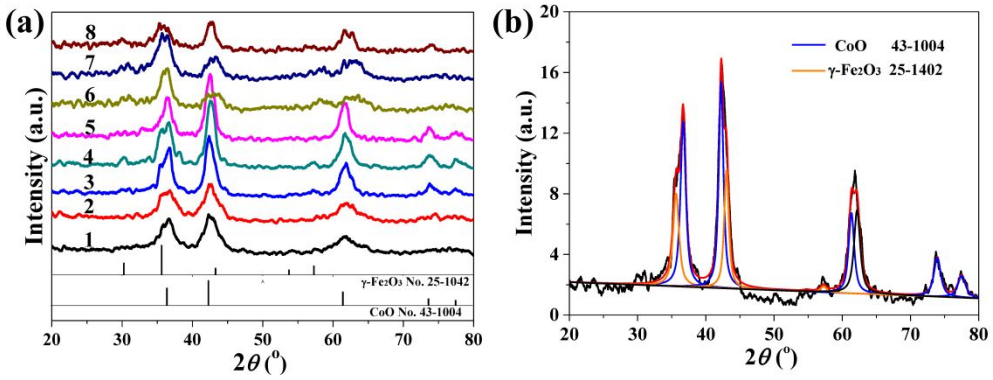

Figure S2. (a) XRD patterns of (1) 0.05, (2) 0.10, (3) 0.20, (4) 0.30, (5) 0.40, (6) 0.60, (7) 0.80, and (8) 1.00Fe-CoO NCs; (b) peak splitting and fitting result for the XRD pattern of 0.15Fe-CoO NCs.

Table S1. The ratios of peak areas due to γ-Fe_2O_3 and CoO in CoO and Fe-CoO.

No.	CoO	0.05	0.1	0.15	0.2	0.3	0.4	0.6	0.8	1.0
γ-Fe_2O_3	0.00	5.13	7.66	10.0	11.5	19.9	27.6	22.6	31.3	35.4
CoO	100	46.1	40.4	45.8	36.6	54.4	55.9	39.5	42.9	37.4
Ratio	0.00	0.11	0.19	0.22	0.31	0.37	0.49	0.57	0.73	0.95

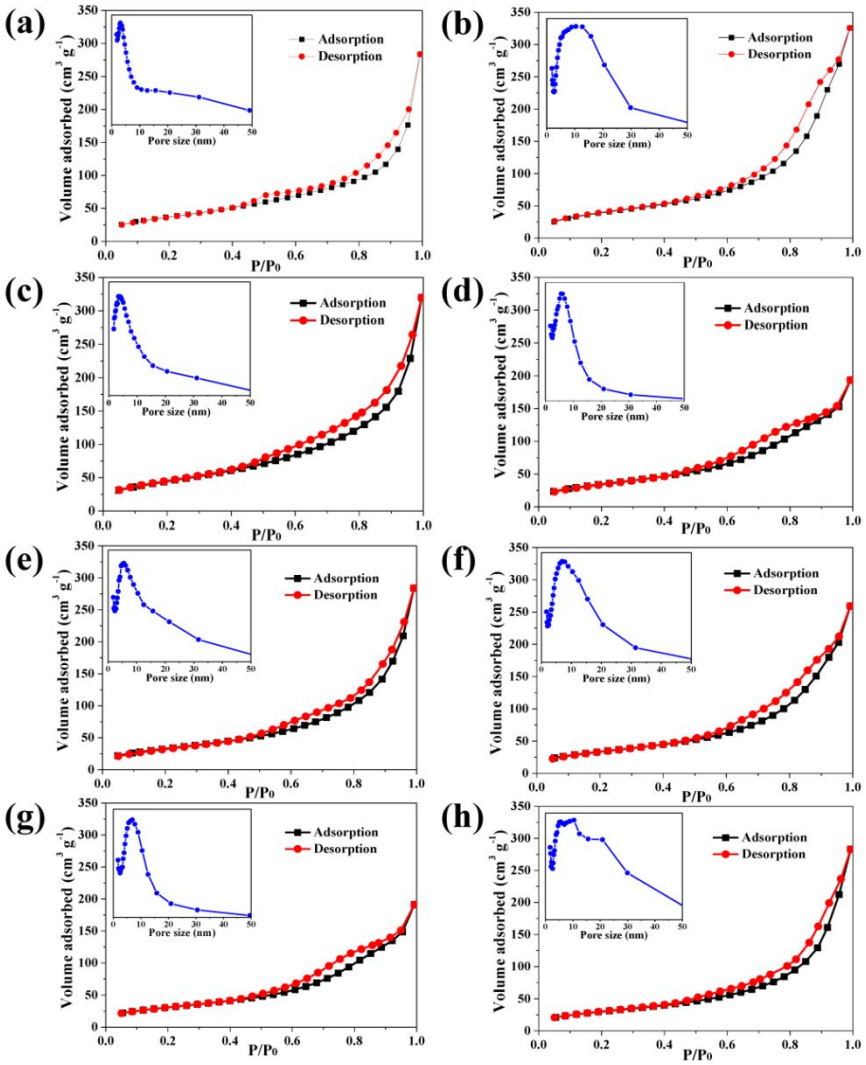

Figure S3. N_2 adsorption/desorption isotherms of (a) 0.05Fe-CoO, (b) 0.1Fe-CoO, (c) 0.20Fe-CoO, (d) 0.3Fe-CoO, (e) 0.4Fe-CoO, (f) 0.6Fe-CoO, (g) 0.8Fe-CoO, (h) 1.0Fe-CoO NCs.

Table S2. Specific surface area (A_{BET}), pore volume (P_V) and average pore size (P_S) of CoO and Fe-CoO.

NO.	A_{BET} (m^2/g)	P_V (cm^3/g)	P_S (nm)
CoO	216.1638	0.882486	14.4553
0.05Fe-CoO	139.0821	0.444407	11.8825
0.10Fe-CoO	146.5244	0.504599	12.4933
0.15Fe-CoO	205.3850	0.655105	11.5848
0.20Fe-CoO	166.1699	0.500521	11.0423
0.30Fe-CoO	129.1306	0.30397	8.4357
0.40Fe-CoO	124.1001	0.44052	12.8422
0.60Fe-CoO	123.5661	0.404191	11.7936
0.80Fe-CoO	113.6521	0.299565	9.5858
1.00Fe-CoO	110.6212	0.440364	14.4259

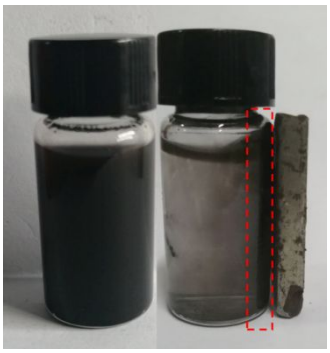

Figure S4. The suspension of 0.15Fe-CoO NCs after ultrasound for 5min (left) and the corresponding state after applying a magnet for 30 min (right).

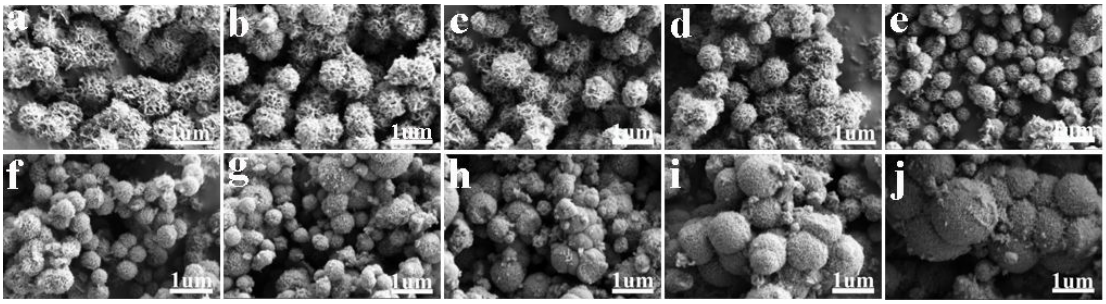

Figure S5. SEM photos of (a) CoO, (b) 0.05, (c) 0.10, (d) 0.15, (e) 0.20, (f) 0.30, (g) 0.40, (h) 0.60, (i) 0.80, and (j) 1.00Fe-CoO NCs.

Table S3. Surface atomic ratios (at.%) of Fe/Co on CoO and Fe-CoO determined by EDS.

No.	CoO	0.05	0.1	0.15	0.2	0.3	0.4	0.6	0.8	1.0
Fe (at.%)	0.00	11.5	16.1	18.4	22.1	25.9	29.7	40.0	45.5	49.1
Co (at.%)	100	88.5	83.9	81.6	77.9	74.1	70.3	60.0	54.5	50.9
Fe/Co (%)	0.00	0.13	0.19	0.23	0.28	0.35	0.42	0.67	0.83	0.97

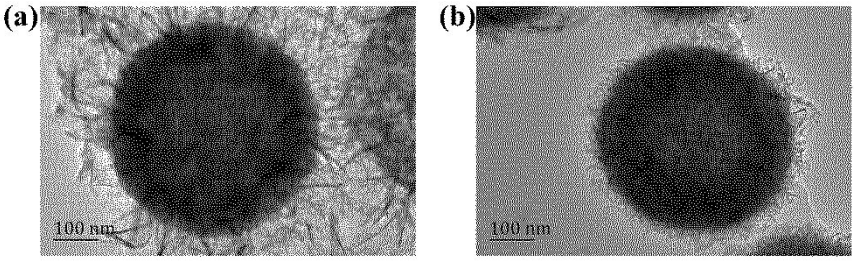

Figure S6. TEM photos of single CoO NP and 0.15Fe-CoO NP.

Table S4. Atomic ratios (at.%) of surface elements on CoO and 0.15Fe-CoO measured by XPS.

No.	Fe^{3+}	Fe^{2+}	Co^{3+}	Co^{2+}	O_α	O_β	O_γ
CoO	0	0	24.9	75.1	43.2	29.0	27.8
0.15Fe-CoO	59.5	40.5	21.1	78.9	53.0	37.3	9.7

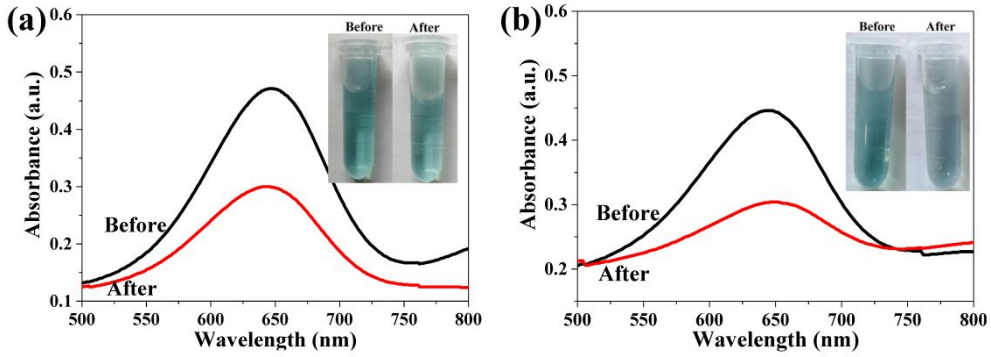

Figure S7. Catalytic oxidation of TMB by (a) CoO NPs and (b) 0.15Fe-CoO NCs without H_2O_2 after high-purity N_2 was continuously purged before reaction.

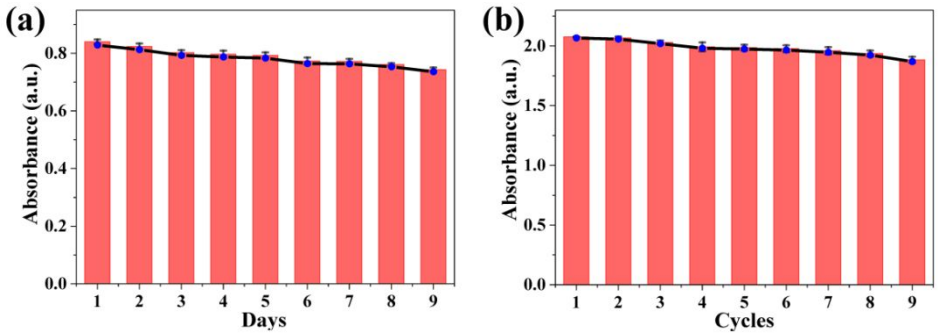

Figure S8. (a) Durability and (b) repeatability performance of 0.15Fe-CoO NCs as peroxidase mimics.

Table S5. Comparison of kinetic parameters of 0.15Fe-CoO, HRP and other peroxidase mimics.

No.	H_2O_2		TMB		Ref.
	K_m (mM)	V_m ($\times 10^{-8}$ M s^{-1})	K_m (mM)	V_m ($\times 10^{-8}$ M s^{-1})	
0.15Fe-CoO NCs	11.2	24.1	0.170	50.9	This work
HRP	3.70	8.71	0.434	10.0	[1]
Fe_3O_4 MNPs	154	9.78	0.098	3.44	[1]
WS_2 NSs	15.2	65.2	0.805	22.0	[2]
$Au_{21}Pd_{79}$ NCs	5.89	8.19	0.295	19.7	[3]
Pd NPs/meso-C	58.0	–	0.130	–	[4]
Cu-Ag/rGO NCs	8.62	7.02	0.634	4.26	[5]
$KFePW_{12}O_{40}$ NPs	165	6.9	0.346	3.7	[6]

Table S6. Comparison of the analytical parameters for H_2O_2 sensing with published reports.

Samples	Method	Time/s	Linear range/μM	LOD/μM	Ref.
0.15Fe-CoO NCs	Colorimetric	60	6–20	4.40	This work
$CePO_4$-CeO_2 NRs	Colorimetric	240	5–150	2.90	[7]
Au-Hg/rGO NCs	Colorimetric	60	5–100	3.25	[8]
NiFe-LDHNS	Colorimetric	600	10–500	4.40	[9]
Au/Co_3O_4-CeO_x NCs	Colorimetric	180	10–100	5.29	[10]
FePt-Au HNPs	Colorimetric	180	20–700	12.33	[11]
Au@Ag NRs	Colorimetric	600	10–10000	6.00	[12]
MOF-808	Colorimetric	1800	10–15000	4.50	[13]
Te@PEDOT NCs	Colorimetric	600	10–100	4.83	[14]
rGO/Cu_8S_5/PPy NSs	Fluorescence	–	0–20	0.688	[15]
FeS (NNs)/GCE	Electrochemical	–	5–140	4.30	[16]
FeSe (NSs)/GCE	Electrochemical	–	5–100	3.00	[16]

Table S7. Comparison of the analytical parameters for DA sensing with published reports.

Samples	Method	Time/s	Linear range/μM	LOD/μM	Ref.
0.15Fe-CoO NCs	Colorimetric	60	2–10	1.99	This work
Co_3O_4@NiO NTs	Colorimetric	400	1–20	1.21	[17]
CuS-BSA-$Cu_3(PO_4)_2$	Colorimetric	1200	0.05–100	0.13	[18]
Cys-AgInZnS QDs	Fluorescence	–	15–120	0.65	[19]
ZnO@Cys NPs	Fluorescence	–	26.3–68.5	0.79	[20]
Pdots@AMP-Cu	Fluorescence	–	10–400	4.00	[21]
Au/RGO/GCE	Electrochemical	–	6.8–41	1.40	[22]
PtTi NPs/GCE	Electrochemical	–	4–500	3.20	[23]
ENA/ITO	Electrochemical	–	0.25–20	0.228	[24]
UiO-66-NH_2@P(ANI-co-ANA)/GCE	Electrochemical	–	10–110	0.30	[25]

References

(1) Gao, L.; Zhuang, J.; Nie, L.; Zhang, J.; Zhang, Y.; Gu, N.; Wang, T.; Feng, J.; Yang, D.; Perrett, S.; Yan, X. Intrinsic peroxidase-like activity of ferromagnetic nanoparticles. *Nat. Nanotechnol.* **2007,** *2* (9), 577-583.

(2) Tang, Y.; Hu, Y.; Yang, Y.; Liu, B.; Wu, Y. A facile colorimetric sensor for ultrasensitive and selective detection of Lead(II) in environmental and biological samples based on intrinsic peroxidase-mimic activity of WS_2 nanosheets. *Anal. Chim. Acta* **2020,** *1106*, 115-125.

(3) Cai, S.; Fu, Z.; Xiao, W.; Xiong, Y.; Wang, C.; Yang, R. Zero-dimensional/ two-dimensional Au_xPd_{100-x} nanocomposites with enhanced nanozyme catalysis for sensitive glucose detection. *ACS Appl. Mater. Interfaces* **2020,** *12* (10), 11616-11624.

(4) Zhang, W.; Niu, X.; Li, X.; He, Y.; Song, H.; Peng, Y.; Pan, J.; Qiu, F.; Zhao, H.; Lan, M. A smartphone-integrated ready-to-use paper-based sensor with mesoporous carbon-dispersed Pd nanoparticles as a highly active peroxidase mimic for H_2O_2 detection. *Sensor. Actuat. B: Chem.* **2018,** *265*, 412-420.

(5) Darabdhara, G.; Sharma, B.; Das, M.; Boukherroub, R.; Szunerits, S. Cu-Ag bimetallic nanoparticles on reduced graphene oxide nanosheets as peroxidase mimic for glucose and ascorbic acid detection. *Sensor. Actuat. B: Chem.* **2017,** *238*, 842-851.

(6) Zeb, A.; Sahar, S.; Qazi, U.; Odda, A.; Ullah, N.; Liu, Y.; Qazic, I.; Xu, A.

Intrinsic peroxidase-like activity and enhanced photo-Fenton reactivity of iron-substituted polyoxometallate nanostructures. *Dalton Trans.* **2018,** *47*, 7344-7352.

(7) Vinothkumar, G.; Lalitha, A.; Suresh Babu, K. Cerium phosphate-cerium oxide heterogeneous composite nanozymes with enhanced peroxidase-like biomimetic activity for glucose and hydrogen peroxide sensing. *Inorg. Chem.* **2019,** *58* (1), 349-358.

(8) Kong, F.; Yao, L.; Lu, X.; Li, H.; Wang, Z.; Fang, H.; Wang, W. Au-Hg/rGO with enhanced peroxidase-like activity for sensitive colorimetric determination of H_2O_2. *Analyst* **2020,** *145* (6), 2191-2196.

(9) Zhan, T.; Kang, J.; Li, X.; Pan, L.; Li, G.; Hou, W. NiFe layered double hydroxide nanosheets as an efficiently mimic enzyme for colorimetric determination of glucose and H_2O_2. *Sensor. Actuat. B: Chem.* **2018,** *255*, 2635-2642.

(10) Liu, H.; Ding, Y.; Yang, B.; Liu, Z.; Liu, Q.; Zhang, X. Colorimetric and ultrasensitive detection of H_2O_2 based on Au/Co_3O_4-CeO_x nanocomposites with enhanced peroxidase-like performance. *Sensor. Actuat. B: Chem.* **2018,** *271*, 336-345.

(11) Ding, Y.; Yang, B.; Liu, H.; Liu, Z.; Zhang, X.; Zheng, X.; Liu, Q. FePt-Au ternary metallic nanoparticles with the enhanced peroxidase-like activity for ultrafast colorimetric detection of H_2O_2. *Sensor. Actuat. B: Chem.* **2018,** *259*, 775-783.

(12) Han, L.; Li, C.; Zhang, T.; Lang, Q.; Liu, A. Au@Ag heterogeneous nanorods as nanozyme interfaces with peroxidase-like activity and their application for one-pot analysis of glucose at nearly neutral pH. *ACS Appl. Mater. Interfaces* **2015,** *7* (26), 14463-14470.

(13) Zheng, H.; Liu, C.; Zeng, X.; Chen, J.; Lu, J.; Lin, R.; Cao, R.; Lin, Z.; Su, J. MOF-808: A metal-organic framework with intrinsic peroxidase-like catalytic activity at neutral pH for colorimetric biosensing. *Inorg. Chem.* **2018,** *57* (15), 9096-9104.

(14) Chi, M.; Nie, G.; Jiang, Y.; Yang, Z.; Zhang, Z.; Wang, C.; Lu, X. Self-assembly fabrication of coaxial te@poly(3,4-ethylenedioxythiophene) nanocables and their conversion to Pd@poly(3,4-ethylenedioxythiophene) nanocables with a high peroxidase-like activity. *ACS Appl. Mater. Interfaces* **2016,** *8* (1), 1041-1049.

(15) Jiang, Y.; Gu, Y.; Nie, G.; Chi, M.; Yang, Z.; Wang, C.; Wei, Y.; Lu, X.

Synthesis of RGO/Cu_8S_5/PPy composite nanosheets with enhanced peroxidase-like activity for sensitive colorimetric detection of H_2O_2 and phenol. *Part. Part. Syst. Char.* **2017,** *34* (3), 1600233.

(16) Dutta, A.; Maji, S.; Srivastava, D.; Mondal, A.; Biswas, P.; Paul, P.; Adhikary, B. Synthesis of FeS and FeSe nanoparticles from a single source precursor: a study of their photocatalytic activity, peroxidase-like behavior, and electrochemical sensing of H_2O_2. *ACS Appl. Mater. Interfaces* **2012,** *4* (4), 1919-1927.

(17) Zhu, Y.; Yang, Z.; Chi, M.; Li, M.; Wang, C.; Lu, X. Synthesis of hierarchical Co_3O_4@NiO core-shell nanotubes with a synergistic catalytic activity for peroxidase mimicking and colorimetric detection of dopamine. *Talanta* **2018,** *181*, 431-439.

(18) Swaidan, A.; Barras, A.; Addad, A.; Tahon, J.; Toufaily, J.; Hamieh, T.; Szunerits, S.; Boukherroub, R. Colorimetric sensing of dopamine in beef meat using copper sulfide encapsulated within bovine serum albumin functionalized with copper phosphate (CuS-BSA-$Cu_3(PO_4)_2$) nanoparticles. *J. Colloid Interface Sci.* **2020,** *582* (Pt B), 732-740.

(19) Liu, Y.; He, X.; Ma, P.; Huang, Y.; Li, X.; Sun, Y.; Wang, X.; Song, D. Fluorometric detection of dopamine based on 3-aminophenylboronic acid-functionalized AgInZnS QDs and cells imaging. *Talanta* **2020,** *217*, 121081.

(20) Lin, J.; Huang, B.; Dai, Y.; Wei, J.; Chen, Y. Chiral ZnO nanoparticles for detection of dopamine. *Mater. Sci. Eng. C* **2018,** *93*, 739-745.

(21) Huang, H.; Bai, J.; Li, J.; Lei, L.; Zhang, W.; Yan, S.; Li, Y. Fluorescence detection of dopamine based on the polyphenol oxidase-mimicking enzyme. *Anal. Bioanal. Chem.* **2020,** *412* (22), 5291-5297.

(22) Wang, C.; Du, J.; Wang, H.; Zou, C.; Jiang, F.; Yang, P.; Du, Y. A facile electrochemical sensor based on reduced graphene oxide and Au nanoplates modified glassy carbon electrode for simultaneous detection of ascorbic acid, dopamine and uric acid. *Sensor. Actuat. B: Chem.* **2014,** *204*, 302-309.

(23) Zhao, D.; Yu, G.; Tian, K.; Xu, C. A highly sensitive and stable electrochemical sensor for simultaneous detection towards ascorbic acid, dopamine, and uric acid based on the hierarchical nanoporous PtTi alloy. *Biosens. Bioelectron.* **2016,** *82*,

119-126.

(24) Ding, H.; Guo, W.; Zhou, P.; Su, B. Nanocage-confined electrochemiluminescence for the detection of dopamine released from living cells. *Chem. Commun.* **2020,** *56* (59), 8249-8252.

(25) Hira, S.; Nallal, M.; Rajendran, K.; Song, S.; Park, S.; Lee, J.; Joo, S.; Park, K. Ultrasensitive detection of hydrogen peroxide and dopamine using copolymer-grafted metal-organic framework based electrochemical sensor. *Anal. Chim. Acta.* **2020,** *1118*, 26-35.